ROFT93－85

あけぼの衛星搭載低周波プラズマ波動観測装置

橋本弘蔵[1] 長野勇[2] 山本正幸[3] 岡田敏美[4] 木村磐根[5] 松本紘[6] 沖秀隆[7]

東京電機大学工学部[1] 金沢大学工学部[2] 三菱電機通信機製作所[3]
富山県立大学工学部[4] 京都大学工学部[5]
京都大学超高層電波研究センター[6] 日本電気コンピュータ技術本部[7]

〒101 東京都千代田区神田錦町 2-2 [1]

あらまし

あけぼの衛星は 1989 年 2 月の打ち上げ以来順調に観測を続けてきている．極域におけるオーロラ粒子加速域の精密観測やそれに関連した磁気圏プラズマの描像を明らかにすることを目的とした衛星である．低周波 (VLF) 波動観測装置は磁気圏における波動粒子相互作用の担い手である波動の観測を行なうものである．VLF 波動のダイナミックスペクトルのみならず，アンテナベクトルインピーダンス，絶対強度測定，伝搬ベクトル方向，ポインティングベクトルの測定を行なえるように設計されており，所期の成果を得てきている．これらを実現するための装置の詳細について述べる．

和文キーワード　VLF エミッション，アンテナベクトルインピーダンス，絶対強度測定，伝搬ベクトル方向

EXOS-D (Akebono) Very Low Frequency Plasma Wave Instruments (VLF)

K. Hashimoto[1] I. Nagano[2] M. Yamamoto[3] T. Okada[4]
I. Kimura[5] H. Matsumoto[6] and H. Oki[7]

Faculty of Engineering, Tokyo Denki University[1] Faculty of Engineering, Kanazawa University[2] Mitsubishi Electric Co., Ltd.[3] Faculty of Engineering, Toyama Prefectural University[4] Faculty of Engineering, Kyoto University[5] Radio Atmospheric Science Center, Kyoto University[6] NEC Corporation[7]

2-2 Kanda-Nishikicho, Chiyoda-ku, Tokyo 101, Japan[1]

Abstract

The Akebono (EXOS-D) satellite launched on February 21, 1989 make successful observations. The objectives of VLF instruments on board the satellite are designed to investigate the behavior of plasma waves associated with accelerated auroral particles, wave-particle interaction mechanisms, and propagation characteristics of whistler-mode waves in the magnetosphere. The instruments are designed to measure not only dynamic spectra of VLF waves, but also their absolute field intensities, wave normal vectors, and Poynting vectors. These measurements have been successfully performed. The present paper describes the instruments in detail.

英文 key words　VLF emissions, Antenna vector impedance, Absolute field intensity, Wave normal vector.

1 Introduction

The Akebono (EXOS-D) satellite was launched on February 21, 1989 from the Kagoshima Space Center in Japan. Its altitudes range from 270 km to 10,500 km and its inclination is 75.1°. The polar-orbiting and sun-pointing satellite investigates energy flow from the magnetospheric tail to the auroral region. To attain this investigation, the following scientific instruments are installed:

1. Electric field detectors (EFD)
2. Magnetic field detectors (MGF)
3. VLF (Very Low Frequency) wave detectors (VLF)
4. Stimulated plasma wave and high frequency plasma wave detectors (PWS)
5. Low energy particle detectors (LEP)
6. Suprathermal ion mass spectrometer (SMS)
7. Thermal electrons (Velocity distribution) detectors (TED)
8. Visible and UV auroral television (ATV)

Their initial scientific results are described in a special issue of the Journal of the Geomagnetism and Geoelectricity [e.g., Oya and Tsuruda, 1989].

The VLF instruments have a wide band receiver (WBA), multi-channel analyzers (MCA), Poynting flux analyzers (PFX), ELF range receivers (ELF), and a vector impedance probe (VIP). The present paper describes these subsystems of the VLF wave detectors in detail and stresses the Poynting flux and wave normal measurement (PFX) system as well as other unique features. Brief introduction of the subsystems and the initial results are described in Kimura et al. [1989]. Scientific results obtained by the instrument are described in the above issue, Geophysical Research Letters [e.g. Yamamoto, et al., 1991], Journal of Geophysical Research [e.g. Sawada, et al., 1993], etc. The VLF instrument is designed to investigate the behavior of plasma waves associated with accelerated auroral particles, wave-particle interaction mechanisms, and propagation characteristics of whistler mode and electrostatic mode waves in the magnetospheric plasma. Two electric field components as well as three magnetic field components in the frequency range from a few Hz to about 20 kHz are measured. In addition to their dynamic spectra, wave normal and Poynting flux directions of these wave phenomena can be obtained by ground data processing in a selected frequency region. The resistance as well as the capacitance of the antenna (sheath impedance) are also measured by occasionally applying a constant current to the electric antennas.

2 Instrument Description

The block diagram of the VLF wave instrument is described in Fig. 1. Each subsystem is explained in the following subsections. Main design policy and constraints are shown below.

1. Since the satellite passes the Van Allen radiation belt, radiation-hardened IC's are used. As to CMOS, only 4000 series were available then as high-reliability products.
2. In order to save power consumption, low supply voltages are used as many as possible. For example, most OP-amps are operated at ± 6 V.

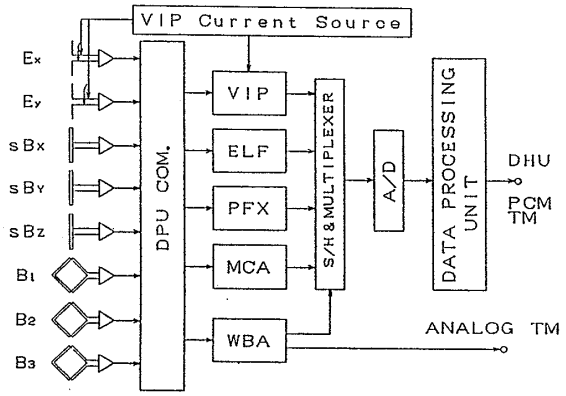

Figure 1: Block diagram of the VLF instrument

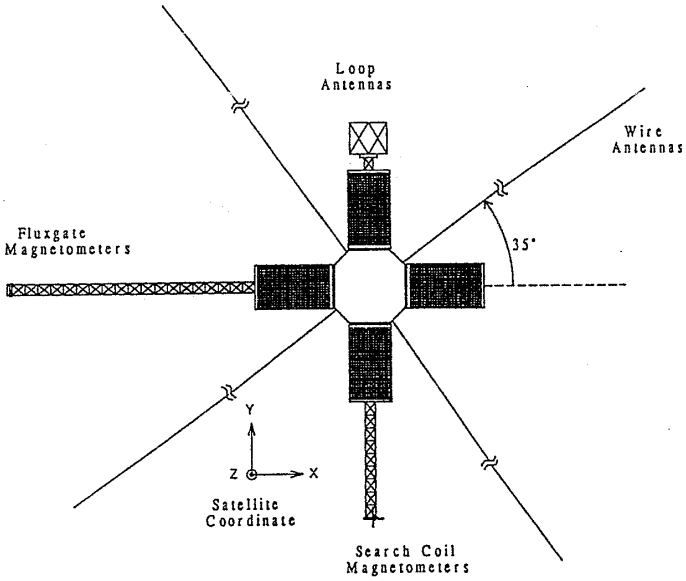

Figure 2: Location of plasma wave sensors

3. PROM (Programmable Read Only Memory) is not allowed to use on board and high-reliability mask ROM is too expensive. Therefore no ROM is used.

2.1 Sensors

The location and orientation of the plasma wave sensors on Akebono are shown in Fig. 2. The spin axis is taken to be the Z axis, which is directed to the sun. The plasma wave sensors consist of:

1. a pair of 60 m tip-to-tip electric dipole wire antennas.
2. three orthogonal magnetic open loop antennas.
3. three orthogonal search coils.

The masts of the loop antennas and the search coils are directed to the positive and negative Y directions, and are 3 m and 6 m long, respectively. The outputs of the search coils are directed to the X-Y-Z axes and called sB_X, sB_Y, and sB_Z, according to the directions of the measured components. The outputs of the open loops are referred to as B_1, B_2, and B_3, and their relation to those of the X-Y-Z

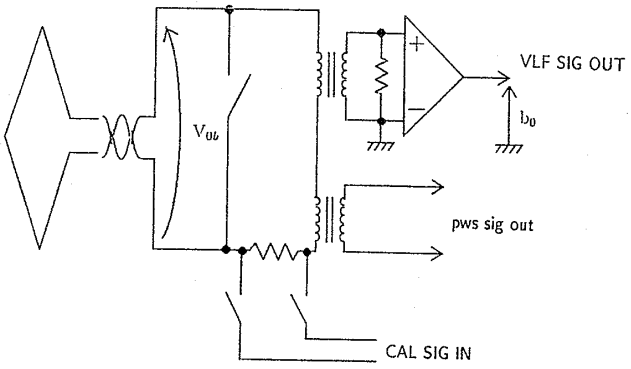

Figure 3: Block diagram of the loop antennas and pre-amplifier

coordinates is,

$$\begin{pmatrix} B_X \\ B_Y \\ B_Z \end{pmatrix} = \begin{pmatrix} -\frac{1}{\sqrt{2}} & \frac{1}{\sqrt{2}} & 0 \\ -\frac{1}{\sqrt{3}} & -\frac{1}{\sqrt{3}} & \frac{1}{\sqrt{3}} \\ \frac{1}{\sqrt{6}} & \frac{1}{\sqrt{6}} & \frac{2}{\sqrt{6}} \end{pmatrix} \begin{pmatrix} B_1 \\ B_2 \\ B_3 \end{pmatrix}.$$

The wire antennas are in the X-Y plane, but its x-axis is 35° off from the X axis as shown in the figure. The two electric field components are called E_x and E_y. The rectangular coordinate systems for these three types of antennas are different as shown above.

The open loop antennas are rectangular (60 cm × 60 cm) coils with 10 turns, and are shared with the PWS instruments [Oya et al., 1990]. Its block diagram is shown in Fig. 3. Special care is taken in order to obtain good sensitivities in both VLF band (for the VLF instrument) and MF band (for the PWS instrument). The small loop antenna is followed by a network with two transformers, both of which are optimized to pick up the signals at lower and higher frequencies, respectively [Okada et al., 1987]. The magnetic field detection threshold level is 0.02 pT/$\sqrt{\text{Hz}}$ at 1 kHz. Calibration is performed by applying the calibrating signal (CAL SIG) across the series resistance of the primary circuit. The switch in the center decides whether the calibration is performed with or without the loop antenna.

The search coils, which are mainly used for the reception of the frequencies less than several 100 Hz and shared with the MGF instrument, are composed of 10^5 turns of 50 μm polyurethane wire on a superpermalloy rod of 3 × 3× 300 (mm^3), whose sensitivity is 0.3 pT at 10 Hz [Fukunishi et al., 1990].

The sensitivity of the magnetic sensors is shown in Fig. 4 in terms of the effective length [Kimura et al., 1990]. Especially the sensitivity of the VLF loop antennas is as high as the effective length of 1 m at 10 kHz.

2.2 WIDA (Wide dynamic range amplifier) IC

Two special hybrid ICs, WIDA IC and Filter IC, were designed to make the VLF instrument compact. The latter is explained in the next subsection. These ICs are widely used in our system and have contributed to make it small and light.

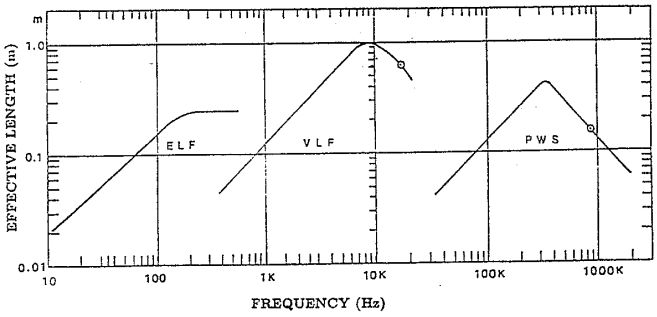

Figure 4: Frequency dependence of the effective length of the loop antennas and search coils [Kimura et al., 1990]

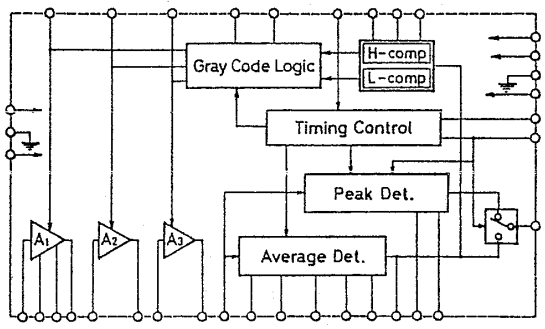

Figure 5: Block diagram of the WIDA IC

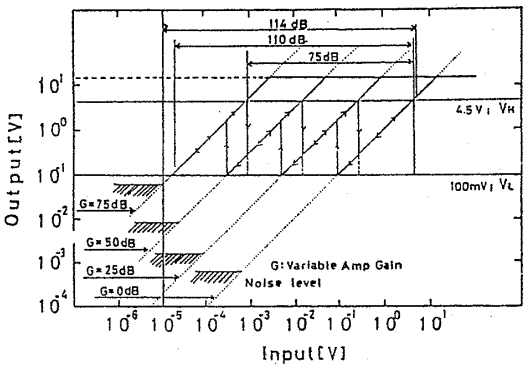

Figure 6: Gain characteristics of the WIDA IC

WIDA IC is a signal detector which has a high resolution of less than 0.1 dB with extremely high dynamic range of 110 dB. This detects both the peak and average value over an adequate period which is controlled by an external clock. Its block diagram is shown in Fig. 5 which composed of the following six blocks;

- VGA (Variable Gain Amplifier)
- AV (Average Detector)
- Peak (Peak Detector)
- Timing control
- Comparator (H-comp and L-comp)
- GCL (Gray Code Logic)

The variable gain amplifier is composed of three OP-amps whose gains are selected independently as either 25 or 0 dB by a signal from the Gray code logic (GCL). This logic has two flip-flops as an Gray code up/down counter. This signal is synchronized with an external timing signal. If an average output is less than the minimum assigned level (for example,

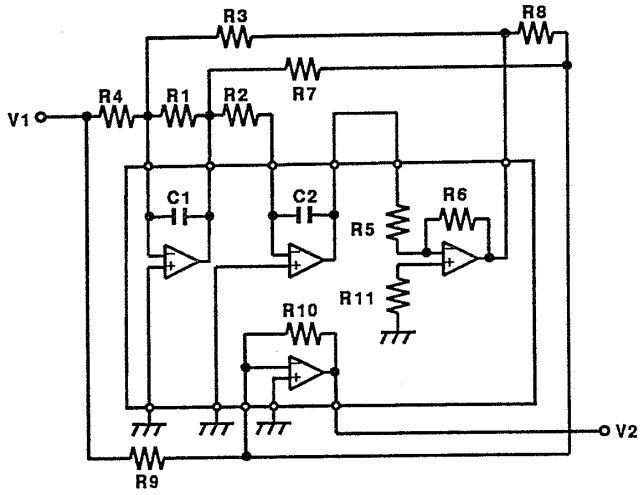

Figure 7: Biquad filter IC

100 mV), the output of the comparator increases the total gain of the WIDA-IC by 25 dB. In contrast, the gain is decreased when the average output exceeds the maximum assigned level (4.5 V). The gain can be selected as 0, 25, 50, or 75 dB. Finally the full dynamic range becomes as much as 114 dB because some hysteresis exist in the system as shown in Fig. 6. At the maximum gain, the gain of all the amplifiers is 25 dB. When the input signal intensity becomes higher, the gain of the amplifier A_1 becomes 0 dB. As the signal becomes higher, the gain of A_2 and A_3 becomes 0 dB in this order.

In our observation, it is very useful to change gains digitally because we can easily estimate real signal intensities. Shortcomings are, however, that it takes some time to change gains in case of sudden signal increases because the changes are made only by the external timing of 0.5 s.

2.3 Filter IC

Because many biquad filters are used in our system, another hybrid IC is designed for this purpose. This IC consists of three low-power quad-OP amps (TL064's) and necessary resistors and capacitors to build the biquad filter. The circuit of one of the three biquad filters is shown in the square box of Fig. 7. The following capacitors and registors are included in this IC: C1 = C2 = 1000 pF, R5 = R6 = R10 = 10 kΩ, and R11 = 5 kΩ. Some Filter IC uses C1 = C2 = 10,000 pF instead of 1000 pF for filters of frequencies less than 1.3 kHz. By adding several resistors on the IC, as shown in the figure, we can make many kinds of filters.

2.4 WBA (Wide band receiver for observation of VLF spectra)

Wide band analogue VLF signals received in the frequency range from 500Hz to 14kHz or 500Hz to 5kHz (selectable by a command) are transmitted to the ground by the analog PM (phase modulation) telemetry. In order to make the carrier tracking on the ground easier, the WBA signals are modulated with a suppressed subcarrier of 20 kHz. Otherwise, low frequency components of the side bands closer to the carrier frequency would disturb the PLL (phase locked loop) of the ground receiver. A VSB (Vestigial Side Band) low-pass filter (−6 dB at 20 kHz) is used to save its bandwidth. In the output of a balanced mixer (analog multiplier) used, almost no original frequency components appeared because of a good isolation between an original signal and the output. This has made a good contribution to the 10.2-kHz Omega signal reception, whose frequency is higher than a half the subcarrier frequency of 20 kHz. [Sawada et al., 1991a]. A 25dB-step four-level automatic gain control is provided by the WIDA IC . A field component to be measured (E_x, E_y, sB_Y or B_2) are selectable by a command.

2.5 MCA (Multi-channel analyzers)

Sixteen MCA channels each for E_x or E_y (selectable by a command) and for sB_Y (chs. 1-10) and B_2 (chs. 11-16) are included in the VLF electronics. The center frequency of each channel is 3.16, 5.62, 10.0, and 17.8 [Hz] ×1, ×10, ×100, and ×1000 with a bandwidth of 30% of the each center frequency. The attenuation at cross-over frequencies between adjacent frequencies is 20 dB. Each channel is composed of the Filter IC for three-stage maximum flat biquad filters and the WIDA IC for the gain control. The maximum allowable input voltage is 1 Vrms and the dynamic range is 80 dB. The MCA is similar to that used by the ISEE satellites etc. [e.g., Gurnett et al., 1978]. The WIDA IC is used for the gain control in our system. The peak and average detector outputs are A/D converted to an 8-bit word and PCM-transmitted with sampling rates of 2, 4, or 1 per sec depend on bit rates; high (64 kbps), medium (16 kbps), and low (4 kbps), respectively. An output example is shown in Kimura et al. [1990].

2.6 PFX (Measurement of wave normal direction and Poynting flux)

Five components of electric and magnetic fields; E_x, E_y, (B_1 or sB_X), (B_2 or sB_Y), and (B_3 or sB_Z) are sent to the ground by the PCM telemetry. The wave normal direction and the Poynting flux of a received signal are calculated on the ground. The reception frequency is either automatically stepped or left fixed at a constant frequency in a frequency range from 100 Hz to 12.75 kHz with a 50-Hz step. The selection of stepped or fixed mode is made by a command while the selection of B or sB is made automatically according to whether the selected reception frequency is higher or lower than 800 Hz. The WIDA IC is also used and the dynamic range of the PFX is also 80 dB. More detailed description is given in the next section.

2.7 ELF (ELF range receiver)

The ELF range receiver is composed of 4 channels: ch. 1; E_x or E_y (selectable by a command), ch. 2; sB_X, ch. 3; sB_Y, and ch. 4; sB_Z. Each channel has an upper cutoff frequency of either 100 or 50Hz, selectable by a command, and a dynamic range of 80 dB. The sampling rate is 320 or 160 Hz and the seventh-order Cauer low-pass filter is used for anti-aliasing. The Bessel type filters was not able to use because of narrow space. Figure 8 shows the characteristic of the low-pass filter of the cutoff frequency of 100 Hz. The

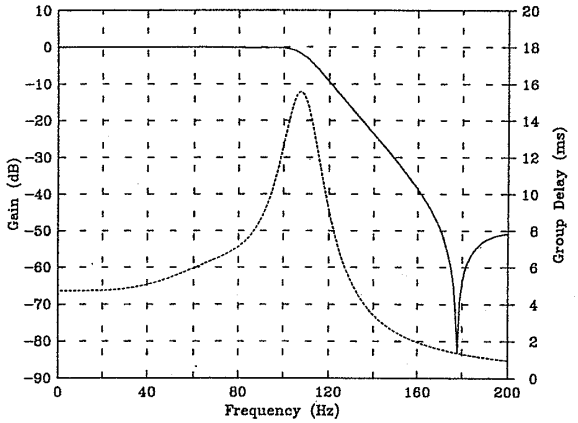

Figure 8: Characteristics of the 100-Hz low-pass filter for ELF

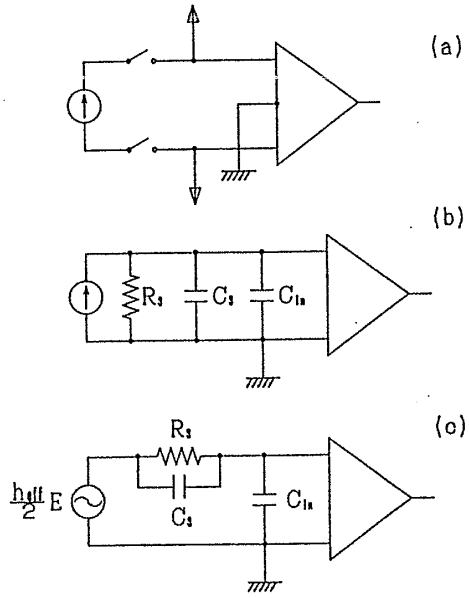

Figure 9: Basic equivalent circuits of VIP

solid line is the gain whose scale is shown in the left and the dashed line shows the group delay time whose scale is in the right. The delay-time characteristics of the Cauer filter is not flat, but satisfactory within the pass band. The outputs of these four channels are simultaneously sampled with 8-bit resolution and telemetered to the ground as a PCM signal. The telemetry word allocation for ELF is four channels for 50 Hz cutoff or two channels for 100 Hz cutoff, but ELF could use four channels for 100 Hz cutoff using PCM words for PFX by changing the RAM contents (cf. subsection 2.9). The wave normal directions and the Poynting flux are then calculated on the ground.

2.8 VIP (Vector impedance probe)

In order to determine the electric field intensity of a signal precisely, the antenna impedance must be known. The basic equivalent circuits of the VIP subsystem is shown in Fig. 9. A constant current source is applied to the input terminals of the wire antennas (Fig. 9a) and the in-phase (I) and quadrature-phase (Q) components of the output with respect to the applied signal are detected by the VIP electronics. An antenna to be measured, either E_x or E_y, is selected by a command. The direct synthesized oscillators (DSOs) are used for the source signal and its quadrature component. The sine wave form is obtained through the use of piecewise linear approximation from a triangular wave because ROM cannot be used. The outputs are applied to the antennas through a 10 M*Omega* resistor as a current source. An intensity of the source is adjusted automatically so as to keep absolute value of the pre-amplifier output voltage constant through a feed-back loop, in order to measure a wide range of the impedance.

The equivalent circuit for one of the two wire antenna elements in a magnetospheric plasma is the sheath resistance R_s and the sheath capacitance C_s in parallel as shown in Fig. 9b. The input capacitance of the pre-amplifier is $C_{\rm in}$, which is known to be 100 pF including the shielded part of the antenna according to the pre-launch measurement. The applied level, which is sampled at 12-bit resolution and log-compressed to 8 bits by a method shown in the next section, and I and Q components are sent to the ground to determine the antenna vector input impedance, or R_s and C_s. The electric field intensity of a wave can be deduced from the sheath impedance, the output voltage, and the total gain of the amplifiers because the equivalent circuit in Fig. 9c. If the electric field intensity is E(V/m) and the effective height of the antenna is $h_{\rm eff}$(m), then the induced voltage for the one element is $Eh_{\rm eff}/2$. This voltage is divided by the sheath impedance and the input impedance [Hashimoto, 1991].

2.9 DPU (Data processing unit)

The main function of DPU is to provide an interface between the spacecraft data handling unit (DHU) and VLF instruments. The DPU provides the control and timing signals for the instrument and send its data to the onboard telemetry system. The DPU has no CPU, but has a 8k-bit RAM (Random Access Memory) as a control memory. Telemetry sequences for different bit rates and formats are stored in the RAM. Each byte stores information on a subsystem, a channel number, analog or digital, log-compressed or not, etc. Command and data from each subsystem are communicated through a kind of bus architecture. The sequences could be changed by rewriting the RAM.

3 PFX (measurement of wave normal direction and Poynting flux)

The PFX is composed of five channels of triple-super-heterodyne receivers with an output bandwidth of 50 Hz. The block diagram is shown in Fig. 10. Lower part of the figure represents the control logic of the WIDA IC. All IF filters are biquad band-pass filters. This system has the following features.

1. In order to make the wave-normal analysis possible, flat time delay, or phase linear filters are used. The first IF filter is the flat-time-delay three-stage band-pass filter [Halpen, 1971], whose characteristics are better than the

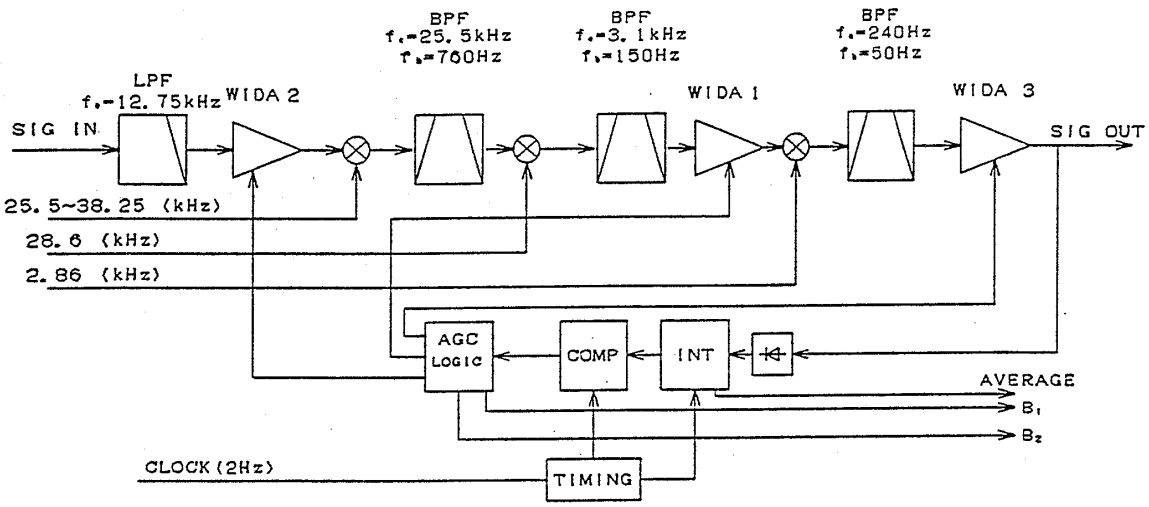

Figure 10: Block diagram of the PFX

conventional one which is frequency-converted from the Bessel low-pass filter (Fig. 11). The biquad filter is composed of the LM101A OP-amps with feed-forward compensation because the IF frequency is 25.5 kHz.

2. The third IF filter is a flat-time-delay six-stage biquad type with two nulls and its pass-band is 240±25 Hz (Fig. 12). At frequencies less than 165 Hz, the attenuation is more than 40 dB and one of the null frequency is close to the sampling frequency of 320 Hz. Generally, signals with frequencies less than 160 Hz are sampled. This system, however, samples signals with frequencies around 240 Hz. Signals from 160 Hz to 320 Hz are effectively converted from 160 Hz to 0 Hz (sampling of bandpass signals). This saves the sampling rate and makes the next IF stage unnecessary. It would be difficult to use the third IF frequency of 80 Hz from the second IF frequency of 3.1 kHz. A very narrow filter would be required.
3. There is a problem when variable gain amplifiers of the WIDA IC is used in the different stages of the heterodyne receiver because the level detection for the gain control is performed at the filterd final output. For example, a strong signal outside of the final bandwidth but inside if the first IF could cause saturation. In order to compromise with this problem, a sequence of gain changes is well contrived. If signal intensities become large, then the gain of WIDA1 (second IF amplifier) becomes 0 dB from the maximum gain operation. At higher signal, the gain of WIDA2 (the amplifier before the first mixer) becomes 0 dB.
4. The signals are sampled at 12-bit resolution and log-compressed to 8 bits. The first bit is the sign bit and the following three bits shows the position of the first '1' in the original 12-bit data. The last four bits are four bits succeeding to the '1'. This system is worse than the 13-bit resolution of the μ law or A law used in the CODEC, but circuits are simpler. Obtained results show that this compression is useful for the later processing on the ground as expected by pre-launch simulations.
5. Direct digital synthesizer is used as the first local oscillator. This can get quick response time. Different

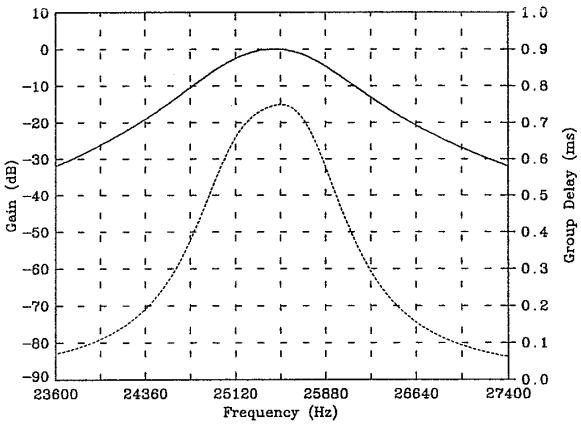

Figure 11: Characteristics of the first IF filter

from a conventional one, ROM for the sine wave form is not used because of the reason stated in Section 2. Triangular wave is generated and filtered. This is sufficient for the present use.

6. On-board caliburation system can put sine waves of not only the center frequency but also the frequency ± 50 Hz. We can monitor the amplitude and phase characteristics of the whole on-board system. Phase differences between the channels were adjusted in less than a few degrees before the launch.

As the frequencies become higher and the Op-amp gain becomes smaller, Q of the biquad filters becomes larger and the characteristics of the filters become different from those of the original design [Thomas, 1971]. The Op-amps with larger gain-bandwidth are used for the first IF. On the other hand, TL061's are used for lower frequency parts to save power. For most of filters, specially designed hybrid-IC's with three TL061's stated in Section 2.3 are used.

4 Results of observations

The satellite and the scientific instruments including the VLF have worked very well. Most of observed results have

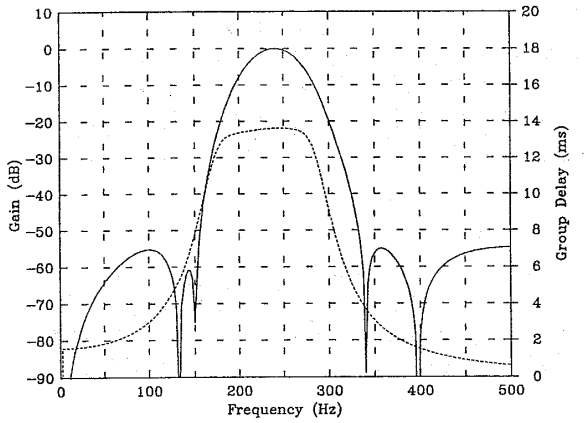

Figure 12: Characteristics of the third IF filter

been published in journals. Initial results of the VLF are presented in Kimura et al. [1990].

The WBA subsystem provides dynamic spectra of VLF waves. Such interesting emissions as whistlers, ELF hiss, auroral hiss, Omega navigation signals, and triggered emissions by the Omega signals [Sawada et al., 1991a] have been observed with high quality. The WIDA system also works well and contributes to estimate the signal amplitude. The gain step of 25 dB happens to be too large considering the dynamic range of the PM analog telemetry. Figure 13 shows an example of dynamic spectra of whistlers in frequencies up tp 15 kHz. This is observed by the open loop antenna for 20 seconds at 1127 UT on March 8, 1989. The satellite was at the altitude of 6000 km and in the geomagnetic latitude of 20°.

The MCA subsystem is mainly used as real-time quick look (QL) at Sagamihara operation center (SOC) of the Institute of Space and Astronautical Science (ISAS). This MCA QL has bad time and frequency resolution, but general features of VLF emissions can be obtained during the satellite tracking.

Poynting vectors and wave normal vectors have successfully been obtained for the Omega signals using the PFX subsystem [Yamamoto, et al., 1991]. Since the Omega signal is a pulse which lasts about one second although the timing of the gain change of WIDA is normally 0.5 second, the whole pulse can not be analyzed. Direction finding of whistles is also performed and reported in Kimura et al. [1990].

Frequency spectra and the four components of ELF emissions observed near the equator are analyzed in frequencies up to several 10 Hz by the ELF subsystem [Sawada, 1991b]. Information on both electric and magnetic field intensities and the wave polarization is used for the analysis.

Antenna impedance has been measured by the VIP subsystem. The impedance is obtained in a complex form and this is essential to estimate the absolute electric field intensities [Hashimoto, et al., 1991].

5 Conclusions

The VLF instruments involve new features and designed under conditions where state-of-the-art ICs can not necessarily be used. They are working very well and satisfactorily. Electric field intensities can be measured very accurately because of well-known amplifier gains by the WIDA, high S/N ratio, and calculation of the pickup factor of the wire antennas by the sheath impedance measurement. The accurate estimation of electric and magnetic field intensity and small phase differences between the channels enable accurate measurements of the wave normal vector, the Poynting vector, the refractive index, etc. The highly sensitive loop antennas as well as the long wire antennas also contribute such data analyses.

Acknowledgments

The Akebono (EXOS-D) project is managed by the Institute of Space and Astronautical Science (ISAS). We thank Meisei Electeric Co. Ltd for the fabrication of the subsystems of the VLF, Nihon Hikoki Co. Ltd. for the fabrication of the masts for the search coils. We are also grateful to colleagues of the Akebono scientific team for their efforts in minimizing RF interference to the VLF instruments.

References

H. Fukunishi, R. Fuji, S. Kokubun, K. Hayashi, T. Tohyama, Y. Tonegawa, S. Okano, M. Sugiura, K. Yumoto, I. Aoyama, T. Sakurai, T. Saito, T. Iijima, A. Nishida, and M. Natori, "Magnetic field observations on the Akebono (EXOS-D) satellite," *J. Geomag. Geoelectr.*, vol. 42, pp. 385–409, 1990.

D. A. Gurnett, F. L. Scarf, R. W. Fredricks, and E. J. Smith, "The ISEE-1 and ISEE-2 Plasma wave investigation," *IEEE Trans. Geosci. Electr.*, vol. GE-16, 225–230, 1978.

P. H. Halpen, "Solution of flat time delay at finite frequencies," *IEEE Trans. Circuit Theory*, vol. CT-18, 241–246, 1971.

K. Hashimoto, I. Nagano, T. Okada, M. Yamamoto, and I. Kimura, "Antenna vector impedance measurement by the EXOS-D (Akebono) Very Low Frequency Plasma Wave Instrument (VLF)," *Geophys. Res. Lett.*, vol. 18, 313–316, 1991.

I. Kimura, K. Hashimoto, I. Nagano, T. Okada, M. Yamamoto, T. Yoshino, H. Matsumoto, M. Ejiri, and K. Hayashi, "VLF observations by the Akebono (EXOS-D) satellite," *J. Geomag. Geoelectr.*, vol. 42, 459–478, 1990.

T. Okada, I. Nagano, K. Hashimoto, I. Kimura, H. Oya, and A. Morioka, "Design of a small loop antenna system for receiving waves in VLF and MF bands using a series-transformer network," *Trans., IEICE*, vol. E70, 550–561, 1987.

H. Oya and K. Tsuruda, "Introduction to the Akebono (EXOS-D) satellite observations," *J. Geomag. Geoelectr.*, vol. 42, 367–370, 1990.

H. Oya, A. Morioka, K. Kobayashi, M. Iizima, T. Ono, H. Miyaoka, T. Okada, and T. Obara, "Plasma wave observation and sounder experiments (PWS) using the Akebono (EXOS-D) satellite—Instrumentation and initial results including discovery of the high altitude equatorial plasma turbulence, *J. Geomag. Geoelectr.*, vol. 42, 411–442, 1990.

A. Sawada, Y. Kishi, M. Yamamoto, A. Sakurai, Y. Kasahara, and I. Kimura, "Propagation characteristics

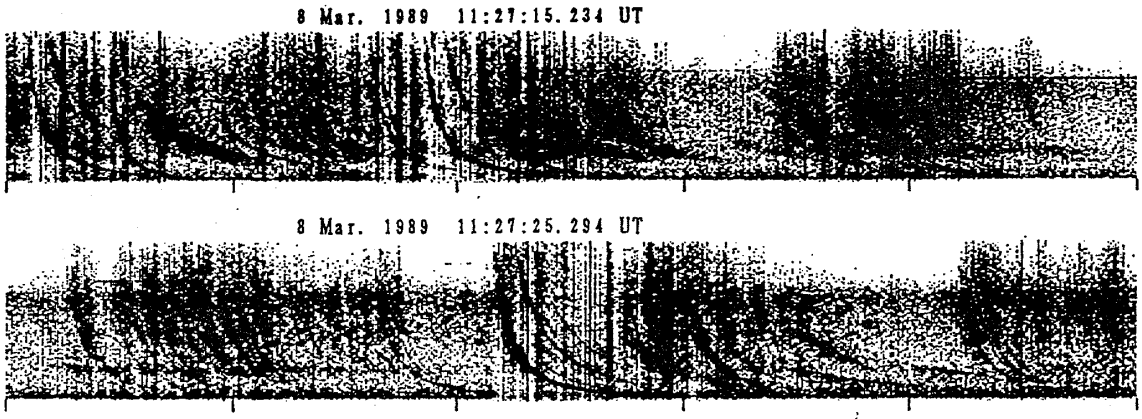

Figure 13: Example of the loop antenna reception (11:27:15 – 11:27:35 UT, March 8, 1989)

of Omega signals and their triggered emissions observed by EXOS-D satellite," *Geophys. Res. Lett.*, vol. 18, 321–324, 1991a.

A. Sawada, Y. Kasahara, M. Yamamoto, I. Kimura, S. Kokubun, and K. Hayashi, "ELF emissions observed by the EXOS-D satellite around the geomagnetic equatorial region," *Geophys. Res. Lett.*, vol. 18, 317–320, 1991b.

A. Sawada, T. Nobata, Y. Kishi, I. Kimura, and H. Oya, "Electron density profile in the magnetosphere deduced from in situ electron density and wave normal directions of Omega signals observed by the Akebono (EXOS D) satellite," *J. Geophys. Res.*, vol. 98, 11,267–11,274, 1993.

L. C. Thomas, The biquad: Part 1— Some practical design considerations, *IEEE Trans. Circuit Theory*, vol. CT-18, 350–357, 1971.

M. Yamamoto, Y. Ito, Y. Kishi, A. Sawada, I. Kimura, I. Nagano, E. Kennai, T. Okada, and K. Hashimoto, "k vector measurements of VLF signals by the satellite EXOS-D," *Geophys. Res. Lett.*, vol. 18, 325–328, 1991.